



# Automatic design of W-operators using membership functions: a case study in brain MRI segmentation

Emilio José Robalino Trujillo<sup>1</sup> · Agustina Bouchet<sup>2</sup> · Virginia Laura Ballarin<sup>1</sup> · Juan Ignacio Pastore<sup>1</sup>

Received: 3 April 2023 / Accepted: 13 March 2024 / Published online: 11 April 2024  
© The Author(s) 2024

## Abstract

A W-operator is an image transformation that is locally defined inside a window W, invariant to translations. The automatic design of the W-operators consists of the design of functions, whose domain is a set of patterns or vectors obtained by translating a window through training images and the output of each vector is a class or label. The main difficulty to consider when designing W-operators is the generalization problem that occurs due to lack of training images. In this work, we propose the use of membership functions to solve the generalization problem in gray level images. Membership functions are defined from the training images to model regions that are often inaccurate due to ambiguous gray levels in the images. This proposal was applied to brain magnetic resonance image segmentation to test its performance in a field of interest in biomedical images. The experiments were carried out with different numbers of training and test images, windows sizes of  $3 \times 3$ ,  $5 \times 5$ ,  $7 \times 7$ ,  $11 \times 11$ , and  $15 \times 15$ , and images with noise levels at 0, 1, 3, 5, 7, and 9%. To calculate the performance of each designed W-operator, the classification error, sensitivity, and specificity were used. From the experimental results, it was concluded that the best performance is achieved with a window of size  $3 \times 3$ . In images with noise levels from 1 to 5%, the classification error is less than 4% and the sensitivity and specificity are greater than 94 and 98%, respectively.

**Keywords** W-operators · Membership functions · Generalization problem · Segmentation · Magnetic resonance images

## 1 Introduction

A W-operator is an image transformation that is locally defined inside a window W, invariant to translations (Benalcázar et al. 2015). Let W be a window that defines a neighborhood of each pixel to process, a W-operator labels each pixel based only on the values observed within the window neighborhood W. The simplest case is when the window

is reduced to a single pixel (Gonzalez and Faisal 2019; Hirata and Papakostas 2021). The machine learning-based approach to designing W-operators consists of estimating the W-operator from collections of input–output image pairs, called training data, that describe the result of the desired transformation. In general terms, learning takes place from patterns or configurations collected from the input images, the training set, and the corresponding values of the points to be analyzed in the ideal images (Hirata and Papakostas 2021; Barrera et al. 2022). The collected patterns determine an estimate of the probability of occurrence of the pair, configuration–output value, that is used to define the W-operator. In this way, the representation of the W-operators is a decision table formed by patterns called observation vectors and their corresponding estimated labels (Guevara et al. 2019).

All the possible observation vectors collected through a window must be represented in the table and must have an associated output value, even those configurations that do not appear in the training images since they may later be present in other images different from the training ones. In this case, the operator must be able to assign a value to them, that is to say, it must be able to generalize (Benalcázar et al.

✉ Agustina Bouchet  
bouchetagustina@uniovi.es

Emilio José Robalino Trujillo  
emilio.jose.robalino.trujillo@gmail.com

Virginia Laura Ballarin  
vballari@fi.mdp.edu.ar

Juan Ignacio Pastore  
jpastore@fi.mdp.edu.ar

<sup>1</sup> Image Processing Lab, ICYTE, UNMDP-CONICET, Mar del Plata, Argentina

<sup>2</sup> Department of Statistics and Operational Research and Mathematics Didactics, University of Oviedo, Oviedo, Spain

2012). However, to complete the table with all the possible configuration vectors, large amounts of training images would be needed but in practice are finite and limited. On the other hand, increasing the window size leads to an exponential increase of the search space and the lack of training images prevents the table being completed with all the possible configurations vectors. For example, with 256 gray levels and a  $3 \times 3$  window, the size of the search space, i.e. the decision table, is equal to  $256^{3 \times 3}$ . The finite and limited number of training images in addition to the exponential increase of the search space when the size of the window increases, both emphasize the generalization problem.

Some works propose several techniques to solve the generalization problem. In Hirata Junior et al. (2002) and Chlapinski and Ciota (2009) the authors use pyramidal multiresolution and aperture to restrict the spatial domain of the windows and the range of gray levels in order to reduce the search size in the designed tables. They apply their proposal in deblurring while in Hirata Jr et al. (2015) authors apply the techniques mentioned above for eyes segmentation on a human face. Other solutions are presented in Benalcázar et al. (2014) and Benalcázar et al. (2015) where W-operators are designed using aperture and feedforward neural networks that model the conditional probability of each observation vector.

On the other hand, in Comas et al. (2014) membership functions are implemented to represent knowledge in a mathematical language based on fuzzy sets theory. Fuzzy sets (FS) take care of the imprecision and the vagueness in human understanding systems and provide a framework to describe, analyze, and understand vague and uncertain events. FS give a theoretical framework to model gray level images because of their imprecision and, also, for predicting unknown values. The imprecision is due to the ambiguity in the gray levels which is generated in the process of capturing the image and the spatial ambiguity caused by the imprecision at the boundaries of objects or the edges in the image. In this way, each region of the image can be modeled as a fuzzy set where the membership function assigns to each pixel a membership degree in the range  $[0,1]$  to solve the ambiguity in the image scene (Acharya and Ray 2005). FS theory is applied in different areas related to image processing. In Huang and Wang (1995), Cheng et al. (1997), Chaira and Ray (2004), Aja-Fernández et al. (2015), Mahajan et al. (2021), membership functions play an important role in finding one or more appropriate threshold values for image segmentation, determining the relationship of a pixel with its membership region. Clustering algorithms are another important task in which FS theory has achieved a good performance. For example, in fuzzy C-means algorithm (FCM) where pixels belong to various clusters with varying membership degrees. This algorithm has been modified in Zhang

and Chen (2004); Yang et al. (2009); Sing et al. (2015); Adhikari et al. (2015) to improve its robustness in the segmentation area.

In this paper, we present a solution to address the generalization problem encountered in the automatic design of W-operators for grayscale images using membership functions. Our method introduces several novel aspects:

- The capability to determine the optimal dimension of the W-operator and the set of weights assigned to each pixel in the image for distinguishing a discrete target set of classes.
- Membership functions are utilized to assign membership degrees to each observation vector not within the domain of the W-operator. Consequently, classes are assigned based on their membership degrees.
- The choice of the type of membership functions employed depends on the nature of the data; that is, any type can be used depending on the dataset.
- We propose the application of this methodology to brain MRI. Nevertheless, it can be applied to any type of image where the segmentation of regions of interest is desired.

The remaining sections of this paper are structured as follows. Section 2 provides an overview of W-operators and membership functions. Section 3 introduces the proposed methodology. Section 4 demonstrates an application of the methodology in brain MRI segmentation. The results and discussion are presented in Sect. 5 and a comparison between the proposed method and other MRI segmentation methods is developed in Sect. 6. Finally, conclusions are drawn in Sect. 7.

## 2 Theoretical framework

In this section, we present some theoretical definitions that provide background and describe the proposed approach.

### 2.1 W-operators

Digital images can be represented by a function  $f : E \rightarrow L$ , where  $E = Z^2$  and  $L = 0, \dots, l - 1$  denotes the set of gray levels of the image. For binary images  $l = 2$  and for grayscale images  $l = 255$  (Hirata and Papakostas 2021). If the set of all images defined on  $E$  with gray levels in  $L$  is denoted as  $L^E$ , an image operator is any mapping of the form  $\Psi : L^E \rightarrow L^E$  (Montagner et al. 2016).

The W-operators are a particular case of image operators, that label each pixel of the image based only on the values observed within the window neighborhood  $W$ . More

information about the functional properties of W-operators can be found in Benalcázar et al. (2012, 2015).

The automatic design of W-operators consists of two stages: a training stage and a testing stage. In the training stage, the W-operator called  $\Psi$ , is designed. Thus, a set of pairs of training images ( $O, I$ ) is considered, where  $O : E \subset \mathbb{Z}^2 \rightarrow \{0, 1, \dots, 255\}$  represents the observed images,  $I : E \subset \mathbb{Z}^2 \rightarrow \{1, \dots, c\}$  represents the ideal images and  $c$  is the number of classes. The W-operator  $\Psi$  is defined as a classifier

$$\Psi : X \rightarrow \{1, \dots, c\}, \quad (1)$$

which maps an observation vector  $X = (x_1, \dots, x_k)$  to one of the labels or classes of the set  $\{1, \dots, c\}$ . An observation vector  $X = (x_1, \dots, x_n)$  is a vector composed of  $n$  values, with  $x_k \in L$ , where each value is defined by  $x_k = f(t + w_k)$  (Montagner et al. 2016).

The window  $W$  is translated pixel a pixel through the images  $O$  and  $I$ , simultaneously (Benalcázar et al. 2012). The values of the window  $W$  inside the image  $O$  generates the observation vector  $X$  (see Fig. 1) and the value of the central pixel of the window  $W$  in the image  $I$  gives the label or class. The window  $W$  is translated through the entire set of training images. Each time an observation vector appears, the corresponding label frequency in the table is increased. Finally, the label of each configuration vector is estimated based on the highest frequency value. As we do not always have large amounts of training images, it is difficult to obtain a complete configuration table. Figure 2 shows, as an example, the construction of this configuration table.

Finally, in the testing step, the error of the W-operator designed is estimated and its predictive capacity is evaluated.

## 2.2 Membership functions

Fuzzy logic is a tool that allows to represent knowledge in a mathematical language through the fuzzy sets theory and their membership functions (Comas et al. 2014). The FS theory provides a framework for describing, analyzing and interpreting vague and uncertain events, i.e., to model the

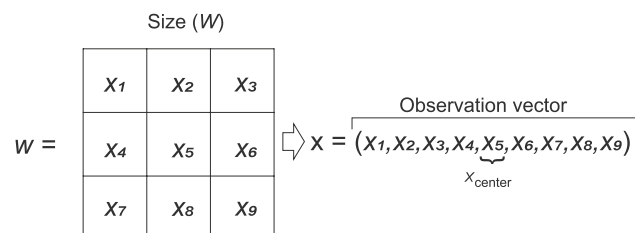


**Fig. 1** Visualization of an observation vector made up of the values within a window

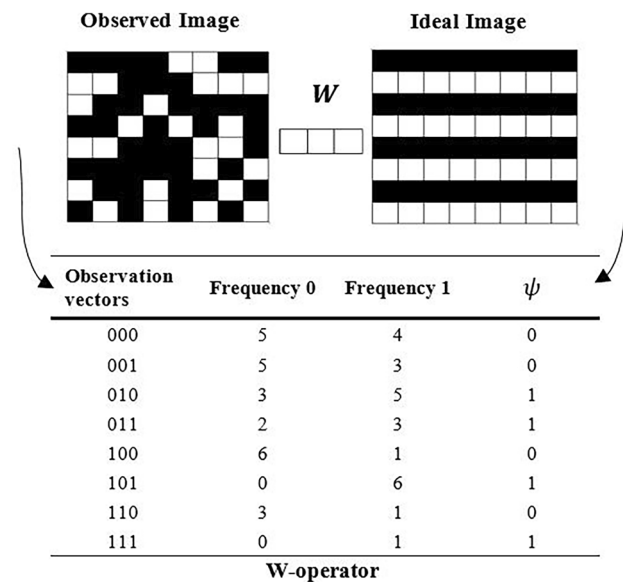


**Fig. 2** Design of a W-operator using a window  $W$  and a pair of training images

imprecision and vagueness existing in human understanding systems. A grayscale image has ambiguity related to the process of capturing images and the spatial ambiguity caused by the imprecision in the objects' boundaries. Each region in the image can be modeled as a FS defined by a membership function, assigning to each pixel a membership degree in the range  $[0, 1]$  (Acharya and Ray 2005). Formally, a membership function for a fuzzy set  $F$  included in  $X$  (universe of discourse), is a map  $\mu(x) : X_F \rightarrow [0, 1]$ , where each element of  $X$  is mapped to a value between 0 and 1. This value quantifies the grade of membership of the element in  $X$  to the fuzzy set  $F$ .

In the context of the automatic design of W-operator, a membership function is defined for each class using the training images. These functions will assign membership degrees to each element of an image within a window, giving rise to a fuzzy window or fuzzy observation vector. Thus, a label according to their membership degrees is assigned to each vector not present in the table designed in the training stage (Robalino et al. 2020). Therefore, membership functions solve the generalization problem present in the automatic design of W-operators for grayscale images.

### 3 Proposed methodology

Due to the lack of training images there will be vectors that will not be found in the configuration table. This lack of predictive capacity of the W-operator designed for the configuration vectors not registered in the training stage is called “generalization problem”. This problem increases the error of the W-operator leading to poor results. We propose the use of membership functions to solve the lack of information produced by the null or low frequency of the observation vectors in the table.

#### 3.1 Definition of membership functions

The membership functions  $u_j$ , for all  $j \in \{1, \dots, c\}$ , are chosen according to each problem and to the nature and type of the data. The construction of membership functions that adequately capture the meanings of the variables has been addressed by several authors (Mendel and Wu 2010; Klir and Yuan 1995). Membership functions can be represented in multiple ways. Due to their mathematical simplicity, the most common are: triangular; trapezoidal, Gaussian, sigmoidal, gamma, among others (Medaglia et al. 2002). Conceptually, there are two approaches to determine the membership function associated with a set. The first approach is based on expert knowledge and the second approach uses a collection of data to design the function. This last approach is used in the automatic design of W-operators, to define the membership functions from a set of training images. Figure 3 shows an example of definition of Gaussian membership function for two classes, from a pair of training images.

In Sect. 4.2 an example of how to determine membership functions based on the problem is introduced.

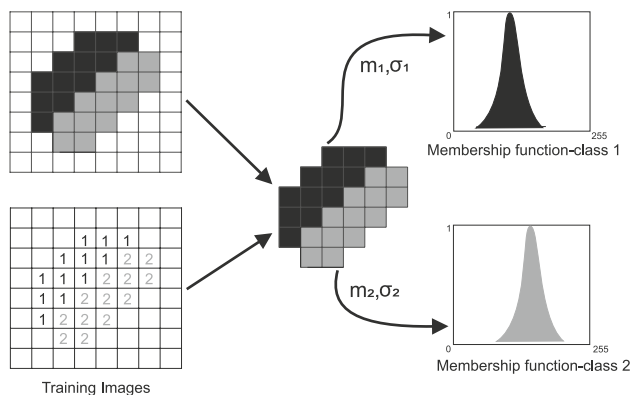


**Fig. 3** Gaussian membership functions for classes 1 and 2 based on a pair of training images

#### 3.2 Design of W-operators by membership functions

The representation of the W-operators is a large decision table where all the possible configurations or observation vectors collected through a window must be represented. Each observation vectors must have an associated output value, even those configurations that do not appear in the training images since they may later be present in other images different from the training ones. In this case, the operator must be able to assign a value to them, that is to say, it must be able to generalize. In this paper, we propose the use of membership functions to solve the generalization problem present in the automatic design of W-operators for gray level images. The membership functions assign membership degrees to each observation vectors not present in the domain of the W-operator.

Each observation vectors is searched in the table generated in the training stage. If the vector appears in the table, then the corresponding label is assigned. Otherwise, the membership functions are used to assign the label. Let  $R_j$  the gray levels range of the the class  $j$ , i.e.,  $R_j = [g_{j_{min}}, g_{j_{max}}]$  where  $g_{j_{min}}$  and  $g_{j_{max}}$  are the minimum and maximum gray level in the  $j$ -class, for all  $j \in \{1, \dots, c\}$ . To calculate the membership degree of the vector  $X$  to the corresponding class  $j$ , first the membership functions are selected from the central pixel  $x_{central}$ . If the value of the central pixel  $x_{central}$  belongs to  $R_j$  then the membership function  $U_j$  is applied to the observation vector  $X$ . If the value of the central pixel  $x_{central}$  belongs to the range of two or more classes, the membership functions of those classes are applied to each of the gray values of the observation vector, and then the average of the degrees of membership is calculated as shown in the following equation:

$$U_j(X) = \frac{\sum_{i=1}^k u_j(x_i)}{k} \quad (2)$$

where  $k$  is the size of the observation vector  $X$ . The assignment of a label to the observation vector will depend on the maximum of the degrees of membership of the analyzed classes.

In the next section we apply our proposed approach to a MRI segmentation problem to test its performance.

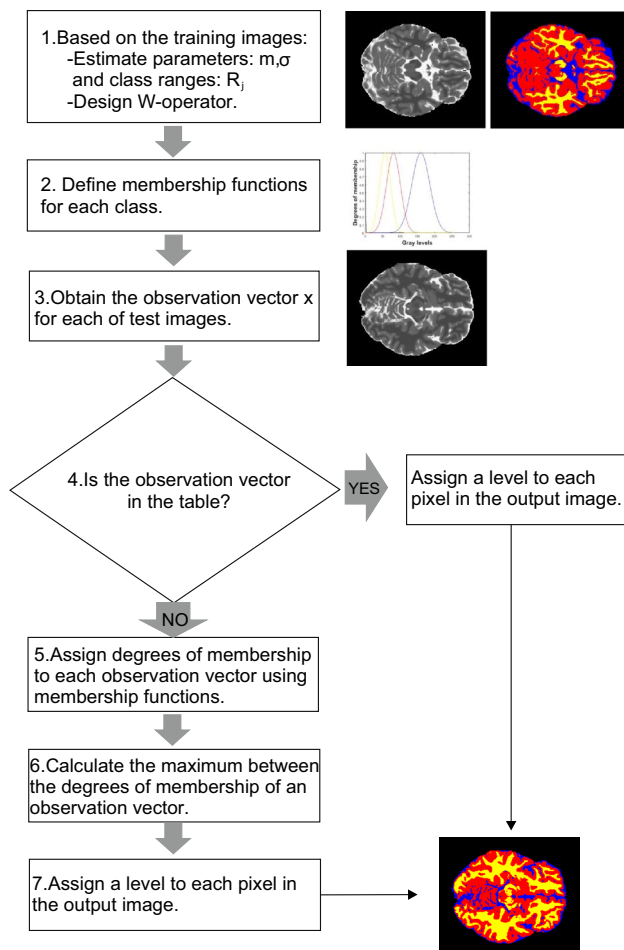


Fig. 4 Diagram of the proposed method

## 4 Application to MRI segmentation

The proposal for design W-operators using membership functions was applied to magnetic resonance images (MRI) segmentation. One of the advantages of MRI is its ability to discriminate various types of tissues for subsequent quantification and, thus, help in the diagnosis of different pathologies. Segmentation of these types of images is a constant requirement in medical science (Meschino et al. 2008). However, one of the main difficulties when working with these images is the overlap between the ranges of gray levels in their tissues, generating fuzzy boundaries between their tissues. This problem increases when MRIs are corrupted by noise, which is unavoidable in these kinds of images. Therefore, the use of membership functions for tissue segmentation in MRI is a good example of the application of our proposal. Figure 4 shows the diagram of the application of the proposed method.

### 4.1 Materials and methods

Simulated 3D images from the Montreal Neurological Institute, McGill University were used (Kwan et al. 1996; Montréal Neurological Institute 2007). From the database, 50 images of size  $271 \times 181$ , weighted in T2 (TR = 3300 ms, TE = 35 ms, 120 ms) were selected. These images contain white Gaussian noise levels at 0, 1, 3, 5, 7, and 9%. The selection criterion was the broad presence of all four tissue types in the simulated brain MRI images.

The most common MRI sequences are T1 and T2-weighted scans. While in T1 images the contrast and brightness of the image are predominately determined by T1 properties of tissue, conversely, in T2 images the contrast and brightness are predominately determined by the T2 properties of tissue. Although images weighted in T2 were used, the proposed method can be applied, without loss of generality, to T1 images. In the case of the latter type of images, there are widely recognized tools and processing software for these images that serve as gold-standard in the neuroimaging research field, such as Computational Anatomy Toolbox for SPM (CAT) (Gaser et al. 2022) and FreeSurfer (Fischl 2012).

We define different experiments to compare the performance of the W-operators. The technical details are described in the following list:

- Images: the noise levels used were 0, 1, 3, 5, 7 and 9%.
- Dataset partition: the dataset is separated in training images and test images. Three partitions were used, in percentage 80-20, 70-30 and 50-50.
- Size windows: five dimensions were used  $3 \times 3$ ,  $5 \times 5$ ,  $7 \times 7$ ,  $11 \times 11$  and  $15 \times 15$ .
- Membership functions: given the nature of the training images, the membership function utilized was the Gaussian membership function.

### 4.2 Definition of membership functions

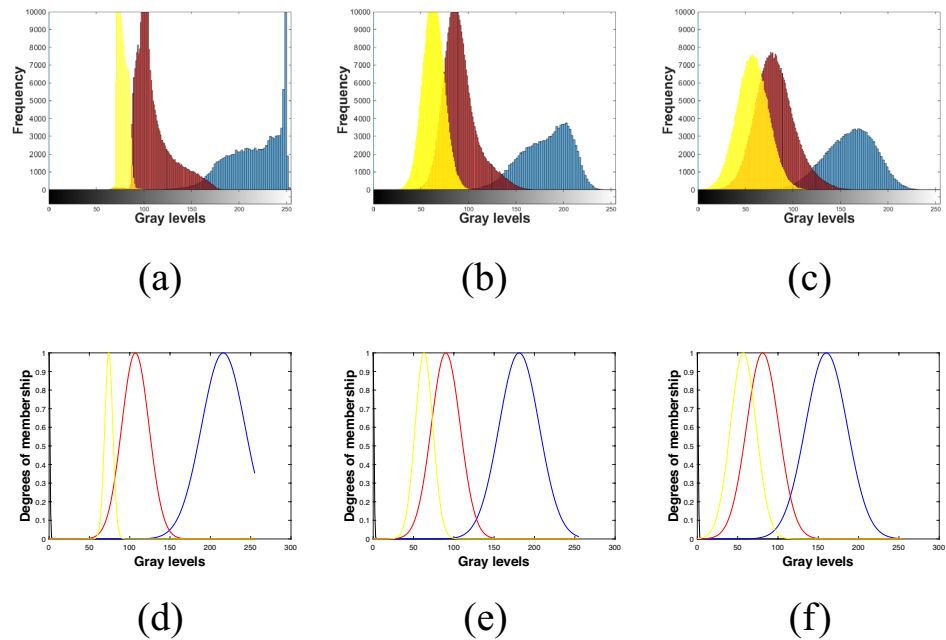
In our experiment, we consider four classes ( $c = 4$ ) since each pixel will be classified into one of the following classes: background, white matter, cerebrospinal fluid, and gray matter.

Gaussian membership functions were chosen based on the shape of the histograms of the different classes, as it can be seen in Fig. 5a–c. These types of membership functions were selected, not only because their capability to adapt to the shape of these specific histograms, but also because their versatility and simplicity.

To define the Gaussian membership functions of each class, background rank  $R_b$ , white matter rank  $R_{wm}$ , cerebrospinal fluid rank  $R_{cf}$ , and gray matter rank  $R_{gm}$  the mean



**Fig. 5** Histograms and Gaussian membership functions using 80-20 dataset partition for the different noise levels. **a–d** 0%. **b–e** 5%. **c–f** 9%



and the standard deviation must be calculated (Comas et al. 2014). Figure 5d–f shows these functions and how they cover the frequency distribution of the gray levels for each class. The gray matter is represented with the color red, the cerebrospinal fluid with blue color, the white matter with yellow color and the background with black color. This last class is not visible because their mean is equal to 0.

For each image  $O_i$  and each gray levels range  $R_j$ , the mean  $m_{ij}$  and the standard deviation  $\sigma_{ij}$  are determined. Once the estimation of the parameters  $m_{ij}$  and  $\sigma_{ij}$  have been calculated, the average for each class  $j = \{1, \dots, c\}$  is calculated using the following equations:

$$\bar{m}_j = \sum_{i=1}^N \frac{m_{ij}}{N} \quad \bar{\sigma}_j = \sum_{i=1}^N \frac{\sigma_{ij}}{N}. \quad (3)$$

The Gaussian membership functions for each class are defined using the parameters  $\bar{m}_j$  and  $\bar{\sigma}_j$ . Therefore, four membership functions  $U_b$ ,  $U_{wm}$ ,  $U_{cf}$  and  $U_{gm}$  are established for the background, white matter, cerebrospinal fluid, and gray matter, respectively.

The proposed approach is presented in the pseudocode given in Algorithm 1.

#### Algorithm 1 Proposed algorithm to design W-operators

---

**Require:** Training image set  $D = \{(O_i, I_i)\}_{i=1}^N$ ;  
 Test image set  $D_{test} = \{(O'_i, I'_i)\}_{i=1}^{N'}$ ; Window  $W$

**Ensure:** Test images processed by  $\Psi$

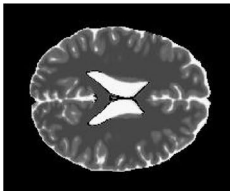
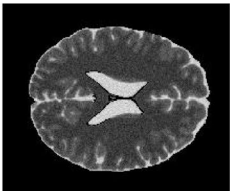
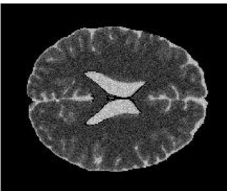
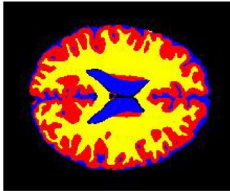
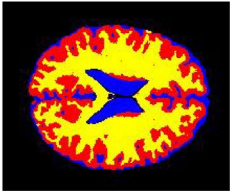
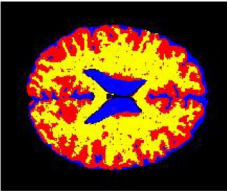
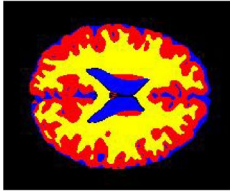
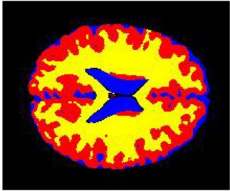
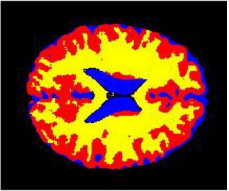
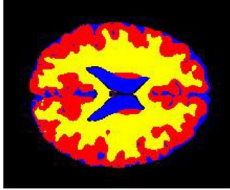
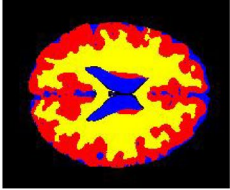
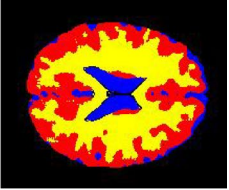
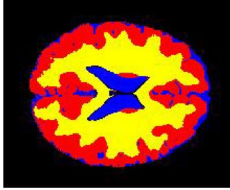
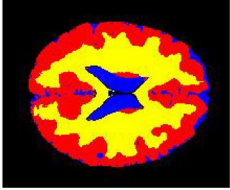
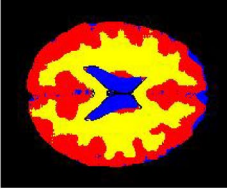
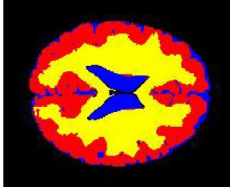
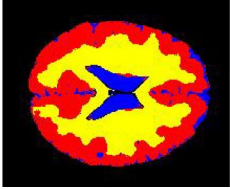
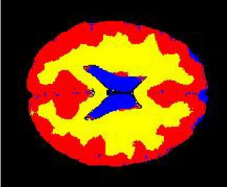
- 1: **for**  $i = 1$  to  $N$  **do**
- 2:   The W-operator  $\Psi$  is designed using  $D$  and  $W$
- 3: **end for**
- 4: The Gaussian functions  $U_j$  are defined from  $D$
- 5: **for**  $i = 1$  to  $N'$  **do**
- 6:    $\Psi$  processes the set  $D_{test}$
- 7:   **if**  $X$  is found in  $\Psi$  **then**
- 8:     Assign label  $j$  to  $X$
- 9:   **else**
- 10:      $U_j$  are applied to  $X$  to assign label  $j$
- 11:   **end if**
- 12: **end for**

---

## 5 Results and discussion

In this section we present the results of the robustness analysis performed in order to validate the W-operators defined by membership functions. The metrics used to evaluate the performance of the operators were classification error, sensitivity, and specificity, all calculated from the values of the average confusion matrix of each

**Table 1** Results of the W-operator using  $3 \times 3$ ,  $5 \times 5$ ,  $7 \times 7$ ,  $11 \times 11$  and  $15 \times 15$  windows and the partition 80-20

Noise %	0	5	9
Test Image			
$3 \times 3$			
$5 \times 5$			
$7 \times 7$			
$11 \times 11$			
$15 \times 15$			

experiment. These metrics are calculated with the following equations (Sokolova and Lapalme 2009):

$$\text{Classification Error} = \frac{FP + FN}{TP + FN + FP + TN} \quad (4)$$

$$\text{Sensitivity} = \frac{TP}{TP + FN} \quad (5)$$

$$\text{Specificity} = \frac{TN}{TN + FP} \quad (6)$$

where TP corresponds to true positives, TN to true negatives, FP to false positives, and FN to false negatives.

As an example of the results obtained in the experiments, some tables are shown. In Table 1 the results of the W-operator, using windows of sizes  $3 \times 3$ ,  $5 \times 5$ ,  $7 \times 7$ ,  $11 \times 11$  and  $15 \times 15$ , are presented. Those results are obtained using the partition 80-20. The gray matter is represented with red color, the cerebrospinal fluid with blue, the white matter with yellow and the background with black.

**Table 2** Classification error, sensitivity and specificity for W-operator using the partition 80-20

Partition 80-20				
Noise %	Size (W)	Error	Sensitivity	Specificity
0	3 × 3	2.533	95.878	99.251
	5 × 5	3.798	92.977	98.853
	7 × 7	5.435	90.423	98.331
	11 × 11	8.085	87.162	97.466
	15 × 15	10.106	85.183	96.78
9	3 × 3	5.407	91.851	98.342
	5 × 5	5.355	89.78	98.358
	7 × 7	7.049	85.601	97.825
	11 × 11	10.476	79.228	96.72
	15 × 15	12.985	75.666	95.876

**Table 3** Classification error, sensitivity and specificity for W-operator using the partition 70-30

Partition 70-30				
Noise %	Size (W)	Error	Sensitivity	Specificity
0	3 × 3	2.610	95.951	99.228
	5 × 5	3.912	93.229	98.818
	7 × 7	5.578	90.75	98.286
	11 × 11	8.162	87.643	97.439
	15 × 15	9.967	85.901	96.82
9	3 × 3	5.509	92.016	98.309
	5 × 5	5.447	90.251	98.328
	7 × 7	7.155	86.363	97.791
	11 × 11	10.549	80.324	96.693
	15 × 15	13.009	76.938	95.862

**Table 4** Classification error, sensitivity and specificity for W-operator using the partition 50-50

Partition 50-50				
Noise %	Size (W)	Error	Sensitivity	Specificity
0	3 × 3	2.882	95.665	99.129
	5 × 5	4.298	93.032	98.674
	7 × 7	5.906	90.801	98.153
	11 × 11	8.533	87.83	97.281
	15 × 15	10.473	86.051	96.609
9	3 × 3	6.105	91.639	98.111
	5 × 5	6.079	89.813	98.112
	7 × 7	7.785	86.014	97.56
	11 × 11	11.253	80.022	96.417
	15 × 15	14.012	76.14	95.471

Tables 2, 3, 4 show the classification error, the sensitivity and the specificity using the different partition for the noise level 0% and 9%. The results presented show that the smallest windows provide the better segmentations. The best results are obtained with windows of size 3 × 3 and 5 × 5. As might be expected, when the noise level decrease, the better segmentation results.

Figures 6, 7 and 8 show the classification error, the sensitivity and the specificity graphs of the W-operators designed with windows of sizes 3 × 3, 5 × 5, 7 × 7, 11 × 11 and 15 × 15, using the different sets of training and test images with different noise levels. The graphs show that when the size of the window grow up, the error increase while the sensitivity and the specificity decrease.

For a window of size 3 × 3, the error is less than 3% in all the partitions used when working with images with noise from 0 to 5%. The error is less than 6.2% when noise increase to 9%. The partition 80-20 proved to be the best, despite the percentage of error.

When the noise level increases, there is a greater overlap between the ranges of each region or class, as could be observed in the training images histograms (see Fig. 4). The greatest overlap can be observed between the white matter (yellow line) and the gray matter (red line) classes, while the overlap of the cerebrospinal fluid class (blue line) is slight.

At this point, it is important to know the generalization capacity (GC) of the proposed method. To achieve this goal, it is essential to calculate the total number of observation vectors (total # of X) obtained from the set of test images, and the number of observation vectors that were labeled by the membership functions (# X labeled by MF). Subsequently, these values are substituted into the following equation:

$$GC = \frac{\#X \text{ labeled by MF}}{\text{total \#of X}} \times 100\%. \quad (7)$$

Equation 7 was applied to calculate the generalization percentage of the proposed method in MRI with 0% and 9% noise. The total number of observation vectors obtained from the set of test images is equal to 962,125. In the case of the application of the W-operator designed using Gaussian functions and a 3 × 3 window to MRI with 0% noise, the number of observation vectors labeled by the membership functions is equal to 423,882. Consequently, the generalization percentage was 44.06%. Conversely, when applying this W-operator to MRI with 9% noise, the generalization percentage increases to 48.09%.



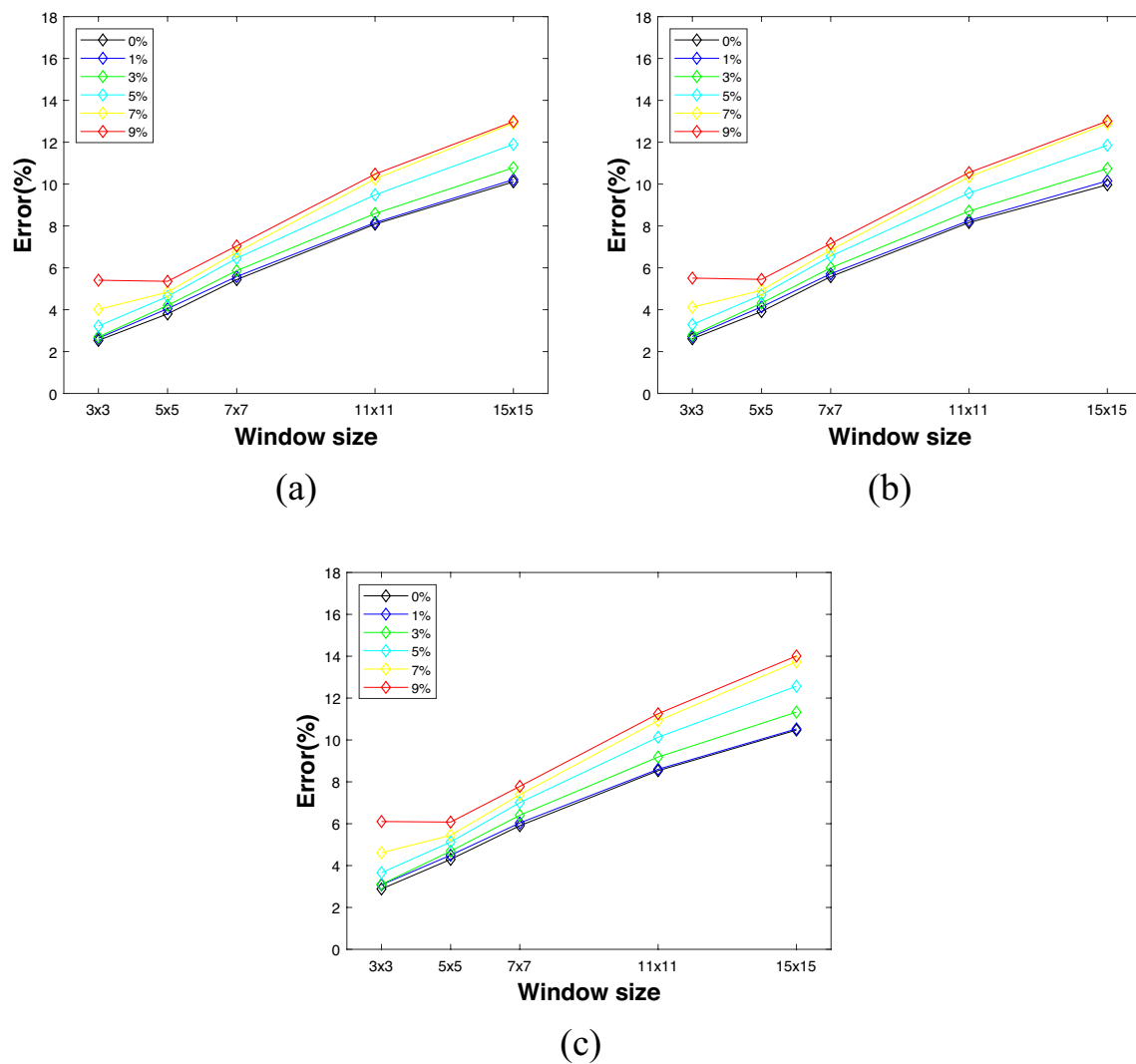


**Fig. 6** Classification error of the W-operators designed for the different partition. **a** 80-20. **b** 70-30. **c** 50-50

It is evident from the generalization percentages in each experiment that the W-operator designed with membership functions demonstrates a higher level of generalization in MRI scenarios characterized by elevated noise levels. This is due to the greater number of new observation vectors that do not exist in the domain of the W-operator under such conditions.

## 6 Comparison of the proposed method with other MRI segmentation methods

The proposed method was compared with other techniques focused on brain MRI segmentation. In Dubey and Mushrif (2015), propose calculating a set of thresholds to segment each tissue in brain MRI, using the intuitionistic diffuse roughness measure (IFRM), obtained using the histogram as a lower approximation and the intuitionistic diffuse hysteron as a top approximation. In Dubey et al. (2016), propose an intuitionistic FCM clustering algorithm for MRI segmentation. The initial centroids are obtained

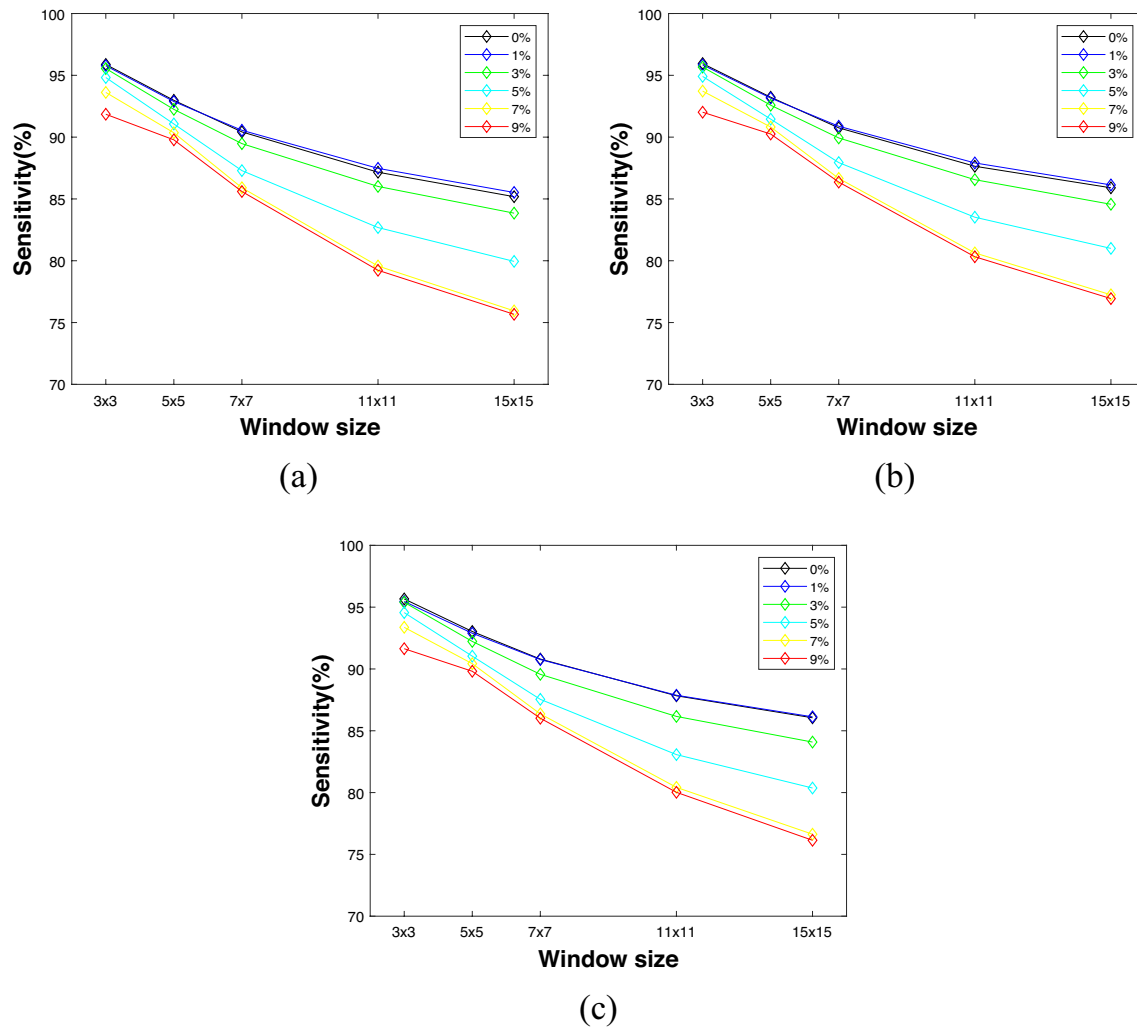


**Fig. 7** Sensitivity of the W-operators designed for the different partition. **a** 80-20. **b** 70-30. **c** 50-50

by means of the aforementioned intuitionistic diffuse roughness measure (RIFCM). In both of these segmentation methods, the evaluation of performance is based on common metrics, including the Jaccard coefficient and the Dice coefficient. These metrics are calculated based on the confusion matrix, composed of true positives (TP), true negatives (TN), false positives (FP), and false negatives (FN). The Jaccard similarity coefficient measures the similarity between two sets by comparing their shared and dissimilar members. Its values range from 0 to 1, with higher values indicating greater similarity between the two sets. The Jaccard coefficient is defined as:

$$\text{Jaccard coefficient} = \frac{TP}{TP + FP + FN}. \quad (8)$$

The Dice coefficient, a measure of similarity between two sets, is defined as:

$$\text{Dice coefficient} = \frac{2 TP}{2 TP + FP + FN}. \quad (9)$$

This similarity metric falls within the range of 0 to 1, and the higher its value, the greater the similarity between the two sets, in this instance, the ideal image and the image segmented by a particular method.

In Table 5, it can be observed that the similarity coefficients evaluated in our methodology exhibit slight discrepancies compared to those obtained by other approaches.

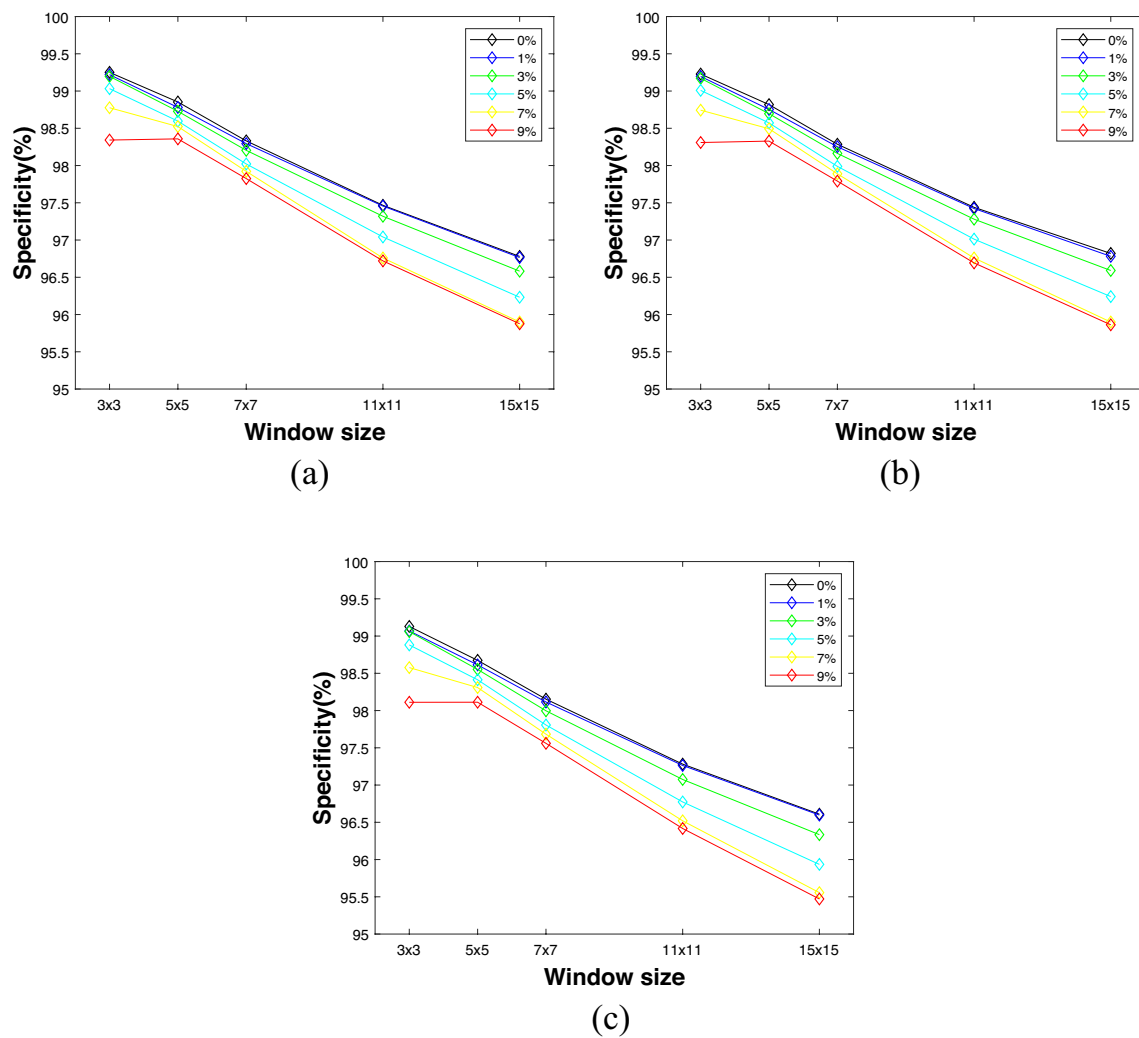


**Fig. 8** Specificity of the W-operators designed for the different partition. **a** 80-20. **b** 70-30. **c** 50-50

**Table 5** Comparison of the proposed method with other methods focused on brain MRI segmentation

Noise %	Tissue class	Jaccard coefficient			Dice coefficient		
		IFRM	RIFCM	WO-MF	IFRM	RIFCM	WO-MF
5	CSF	0.9218	0.9116	0.8448	0.9593	0.9537	0.9157
	GM	0.9186	0.9565	0.8352	0.9576	0.9777	0.9102
	WM	0.9715	0.9456	0.9094	0.9855	0.9720	0.9525
9	CSF	0.8304	0.9016	0.8276	0.9073	0.9482	0.9054
	GM	0.9091	0.9257	0.7362	0.9523	0.9614	0.8481
	WM	0.9554	0.9219	0.8323	0.9772	0.9593	0.9085

Nevertheless, our proposal to utilize membership functions generated from the training data addresses one of the most prominent challenges in the automatic design of W-operators. This challenge lies in generalizing the w-operators

for the processing of new images that were not used during the training phase. As a result, the ability to perform multi-class segmentations is significantly expanded, as illustrated in the case of segmentation in MRI.

## 7 Conclusions

A new approach was introduced for the automatic design of W-operators using membership functions to solve the generalization problem in the case of multi-class segmentation. W-operators designed with the proposed approach were applied to segment magnetic resonance images. The experiments were carried out with different numbers of training and test images, different windows sizes and different noise levels. The error of the designed W-operators increases as the window size increases, obtaining the smallest error for a  $3 \times 3$  window. The classification error also increase as the noise level does.

The proposed method, using membership functions, had good performance in all experiments when working with windows of size  $3 \times 3$ , solving the generalization problem and achieving the segmentation of each tissue in images in gray levels with class ranges with overlap and fuzzy boundaries. As future work, the proposed method will be applied to real magnetic resonance images.

**Acknowledgements** A. Bouchet would like to thank for the support of the Spanish Ministry of Science and Innovation projects PID2022-139886NB-I00.

**Funding** Open Access funding provided thanks to the CRUE-CSIC agreement with Springer Nature.

**Data availability** The datasets used and analyzed during the current study are available at: <https://brainweb.bic.mni.mcgill.ca/brainweb>.

## Declarations

**Conflict of interest** The authors declare that they have no conflicts of interest.

**Humans or animals performed** This article does not contain any studies involving humans or animals performed by any of the authors.

**Open Access** This article is licensed under a Creative Commons Attribution 4.0 International License, which permits use, sharing, adaptation, distribution and reproduction in any medium or format, as long as you give appropriate credit to the original author(s) and the source, provide a link to the Creative Commons licence, and indicate if changes were made. The images or other third party material in this article are included in the article's Creative Commons licence, unless indicated otherwise in a credit line to the material. If material is not included in the article's Creative Commons licence and your intended use is not permitted by statutory regulation or exceeds the permitted use, you will need to obtain permission directly from the copyright holder. To view a copy of this licence, visit <http://creativecommons.org/licenses/by/4.0/>.

## References

Acharya T, Ray AK (2005) Image processing-principles and applications

- Adhikari SK, Sing JK, Basu DK et al. (2015) Conditional spatial fuzzy c-means clustering algorithm for segmentation of mri images. *Appl Soft Comput* 34:758–769
- Aja-Fernández S, Curiale AH, Vegas-Sánchez-Ferrero G (2015) A local fuzzy thresholding methodology for multiregion image segmentation. *Knowl Based Syst* 83:1–12
- Barrera J, Hashimoto RF, Hirata NS et al. (2022) From mathematical morphology to machine learning of image operators. *São Paulo J Math Sci* 16(1):616–657
- Benalcázar M, Brun M, Ballarin V et al. (2012) Automatic design of binary w-operators using artificial feed-forward neural networks based on the weighted mean square error cost function. In: *Progress in pattern recognition, image analysis, computer vision, and applications: 17th theroamerican congress, CIARP 2012, Buenos Aires, September 3–6, 2012. Proceedings 17*. Springer, pp 495–502
- Benalcázar ME, Brun M, Ballarin VL (2014) Automatic design of aperture filters using neural networks applied to ocular image segmentation. In: *2014 22nd European signal processing conference (EUSIPCO)*. IEEE, pp 2195–2199
- Benalcázar ME, Brun M, Ballarin V (2015) Automatic design of window operators for the segmentation of the prostate gland in magnetic resonance images. In: Braidot A, Hadad A (eds) *VI CLAIB 2014*. Springer International Publishing, Cham, pp 417–420
- Chaira T, Ray AK (2004) Threshold selection using fuzzy set theory. *Pattern Recogn Lett* 25(8):865–874
- Cheng HD, Chen C, Chiu H (1997) Image segmentation using fuzzy homogeneity criterion. *Inf Sci* 98(1–4):237–262
- Chlapinski J, Ciota Z (2009) Automated aperture filter design by stochastic optimization. In: *2009 MIXDES*. IEEE, pp 607–612
- Comas DS, Meschino GJ, Brun M et al. (2014) Label-based type-2 fuzzy predicate classification applied to the design of morphological w-operators for image processing. In: *First Latin American congress on computational intelligence*, pp 55–60
- Dubey YK, Mushrif MM (2015) Intuitionistic fuzzy roughness measure for segmentation of brain mr images. In: *2015 ICAPR*. IEEE, pp 1–6
- Dubey YK, Mushrif MM, Mitra K (2016) Segmentation of brain mr images using rough set based intuitionistic fuzzy clustering. *Bio-cybern Biomed Eng* 36(2):413–426
- Fischl B (2012) Freesurfer. *Neuroimage* 62(2):774–781
- Gaser C, Dahnke R, Thompson P et al. (2022). Cat—a computational anatomy toolbox for the analysis of structural mri data. <https://doi.org/10.1101/2022.06.11.495736>
- Gonzalez R, Faisal Z (2019) *Digital image processing second edition*
- Guevara S, Robalino E, Bouchet A et al. (2019) Diseño automático de un clasificador para filtrado de ruido en imágenes binarias utilizando análisis discriminante lineal. *DIIT* 4(1):1–9
- Hirata N, Papakostas G (2021) On machine-learning morphological image operators. *Mathematics* 9:1854
- Hirata Junior R, Brun M, Barrera J et al. (2002) Multiresolution design of aperture operators. *J Math Imaging Vis* 16:199–222
- Hirata Jr R, Dougherty E, Barrera J (2015) Design of gray-scale non-linear filters via multiresolution apertures. In: *European signal processing conference 2015*
- Huang LK, Wang MJJ (1995) Image thresholding by minimizing the measures of fuzziness. *Pattern Recogn* 28(1):41–51
- Klir GJ, Yuan B (1995) Fuzzy sets and fuzzy logic: theory and applications
- Kwan RKS, Evans AC, Pike GB (1996) An extensible mri simulator for post-processing evaluation. In: *International conference on visualization in biomedical computing*, Springer, pp 135–140
- Mahajan S, Mittal N, Pandit AK (2021) Image segmentation using multilevel thresholding based on type ii fuzzy entropy and marine predators algorithm. *Multimed Tools Appl* 80:19335–19359

- Medaglia AL, Fang SC, Nuttle HL et al. (2002) An efficient and flexible mechanism for constructing membership functions. *Eur J Oper Res* 139(1):84–95
- Mendel J, Wu D (2010) Perceptual computing: aiding people in making subjective judgments
- Meschino GJ, Andrade RE, Ballarin VL (2008) A framework for tissue discrimination in magnetic resonance brain images based on predicates analysis and compensatory fuzzy logic. *IC-MED* 2(3):207–222
- Montagner IS, Hirata NS, Hirata R (2016) Image operator learning and applications. In: 2016 29th SIBGRAPI. IEEE, pp 38–50
- Montréal Neurological Institute MU (2007) MNI's BrainWeb dataset
- Robalino E, Pastore JJ, Ballarin V, et al. (2020) Diseño automático de w-operadores mediante el uso de funciones de pertenencia para la segmentación de leucocitos. In: 2020 IEEE ARGENCON. IEEE, pp 1–6
- Sing JK, Adhikari SK, Basu DK (2015) A modified fuzzy c-means algorithm using scale control spatial information for mri image segmentation in the presence of noise. *J Chemom* 29(9):492–505
- Sokolova M, Lapalme G (2009) A systematic analysis of performance measures for classification tasks. *Inf Process Manag* 45(4):427–437
- Yang Z, Chung FL, Shitong W (2009) Robust fuzzy clustering-based image segmentation. *Appl Soft Comput* 9(1):80–84
- Zhang DQ, Chen SC (2004) A novel kernelized fuzzy c-means algorithm with application in medical image segmentation. *Artif Intell Med* 32(1):37–50

**Publisher's Note** Springer Nature remains neutral with regard to jurisdictional claims in published maps and institutional affiliations.